Support information

Water-soluble, Adhesive and 3D Cross-linked Polyelectrolyte Binder for High-performance Lithium-sulfur Battery

*Mingnan Li[1], Jun Zhang[1], Yang Gao, Xiwen Wang, Yan Zhang, and Shiguo Zhang**

College of Materials Science and Engineering, Hunan University, Changsha 410082, Hunan, China

E-mail: zhangsg@hnu.edu.cn

[1]These authors contributed equally to this work.

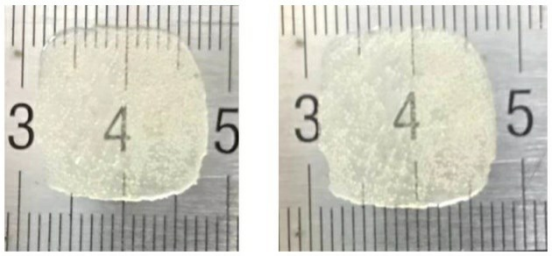

Figure S1. D-PAA/C-EA film before (left) and after (right) immersion in LiTFSI in DOL:DME (1:1, v/v) for 96 h.

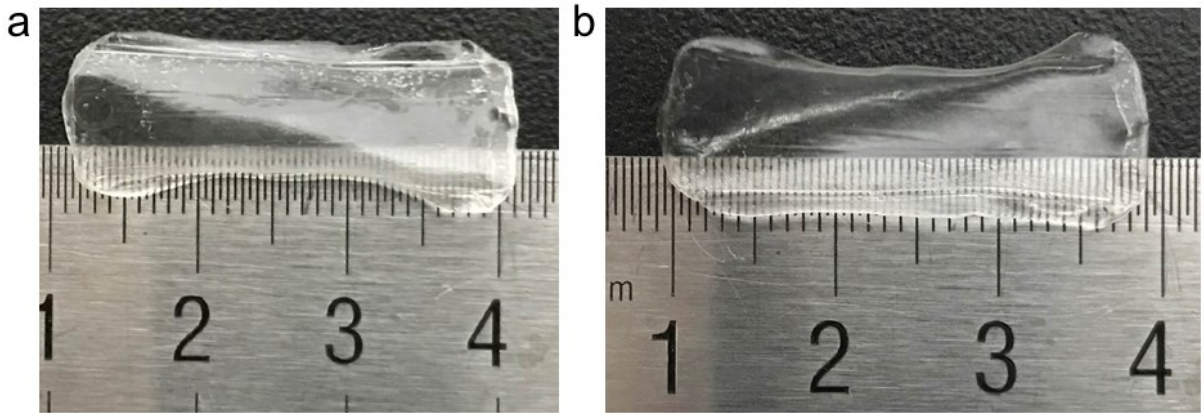

Figure S2. D-PAA/C-EA film (a) before and (b) after immersion in the Li_2S_6-containing Li-S electrolyte (0.5 M Li_2S_6) for 96 h.

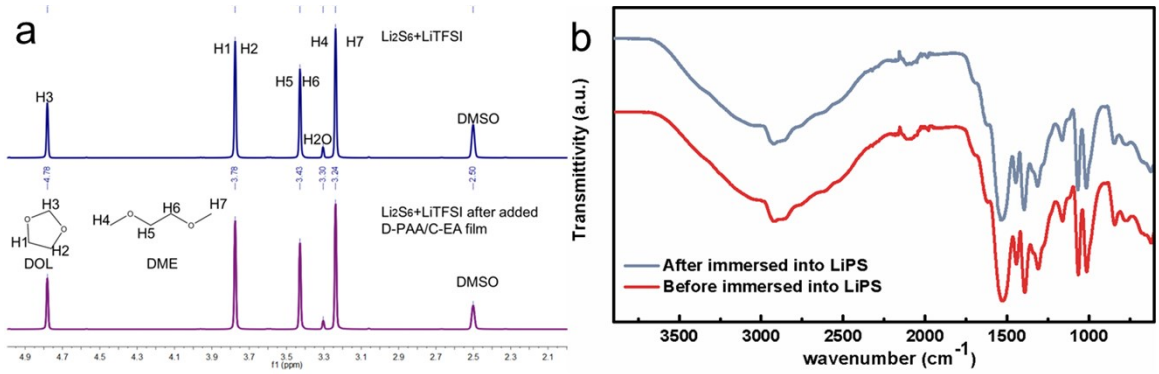

Figure S3. (a) ^{1}H NMR spectra of 0.5 M Li_2S_6-containing Li-S electrolytes and (b) FTIR spectra of D-PAA/C-EA film after immersion test.

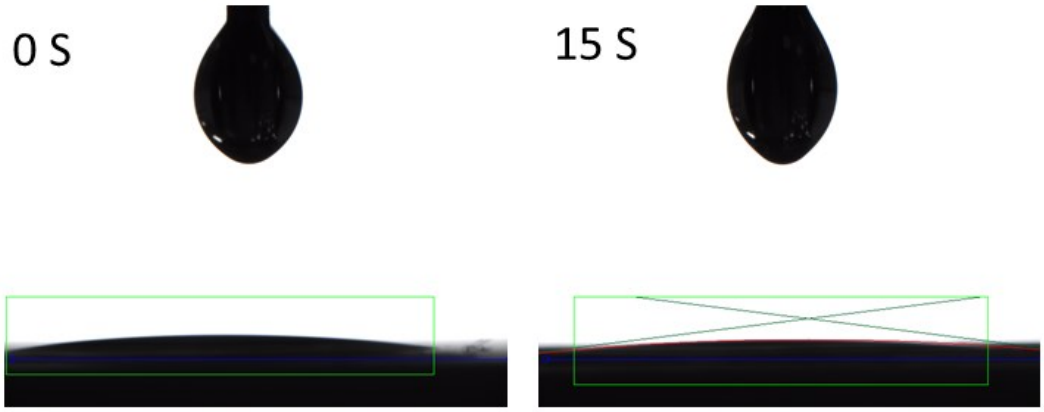

Figure S4. Contact angles of DOL: DME (1:1, v/v) on D-PAA/C-EA coated glass plate.

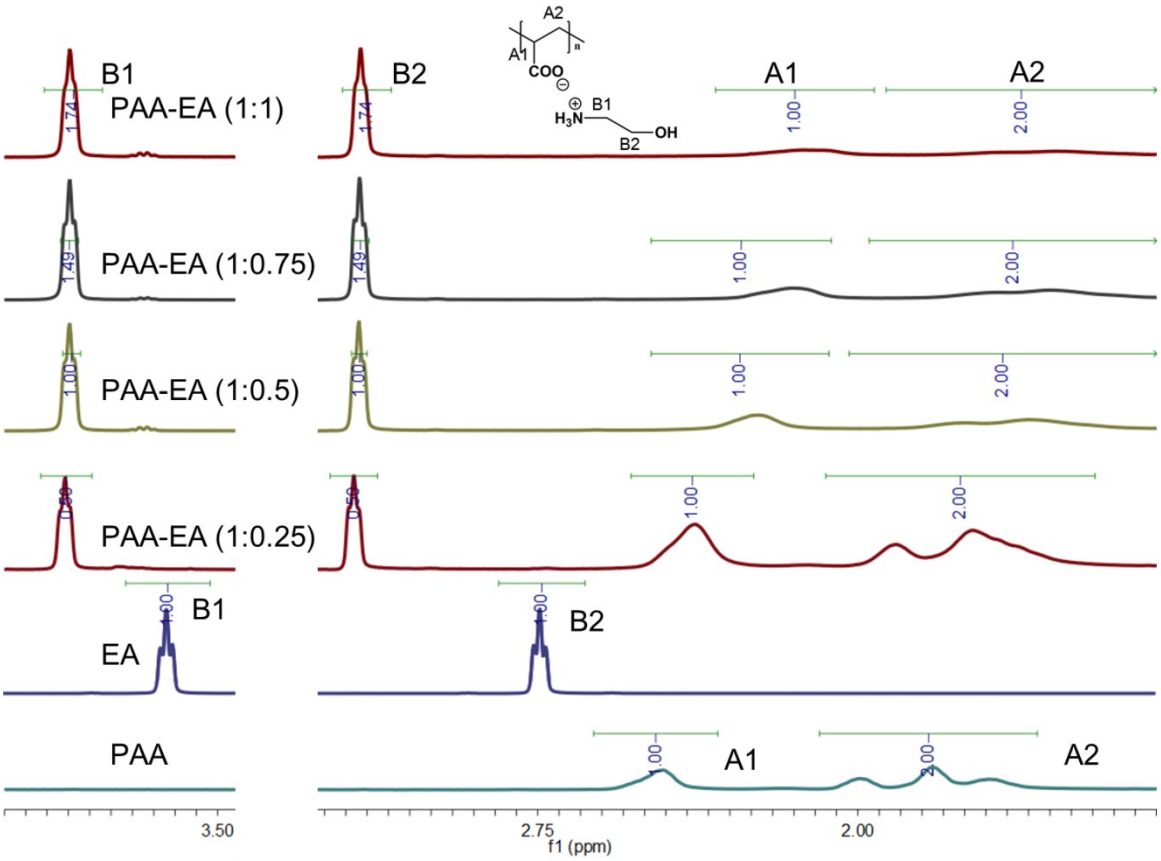

Figure S5. ^{1}H NMR spectra of D-PAA/C-EA binders with variable PAA/EA ratio.

Table S1. The degree (x) of deprotonation of -COOH for D-PAA/C-EA binders with variable PAA/EA ratio.

Sample (m:n)	Integral area $_{B1}$	Integral area $_{A2}$	x (%)
PAA-EA (1:0.25)	0.50	2.00	25.00%
PAA-EA (1:0.5)	1.00	2.00	50.00%
PAA-EA (1:0.75)	1.49	2.00	74.50%
PAA-EA (1:1)	1.74	2.00	87.00%

Since atom number is proportional to the integral peak area, the degree of deprotonation of the carboxyl group (x) can be calculated, according to follow equation:

$$x = \text{Integral area}_{B1} / \text{Integral area}_{A2}$$

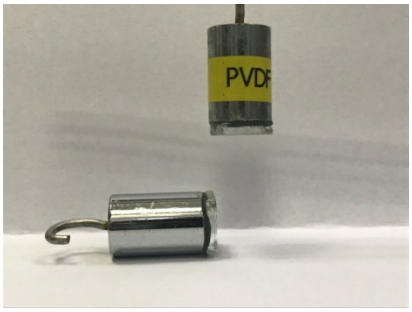

Figure S6. PVDF cannot link the interface of two weights (50 g).

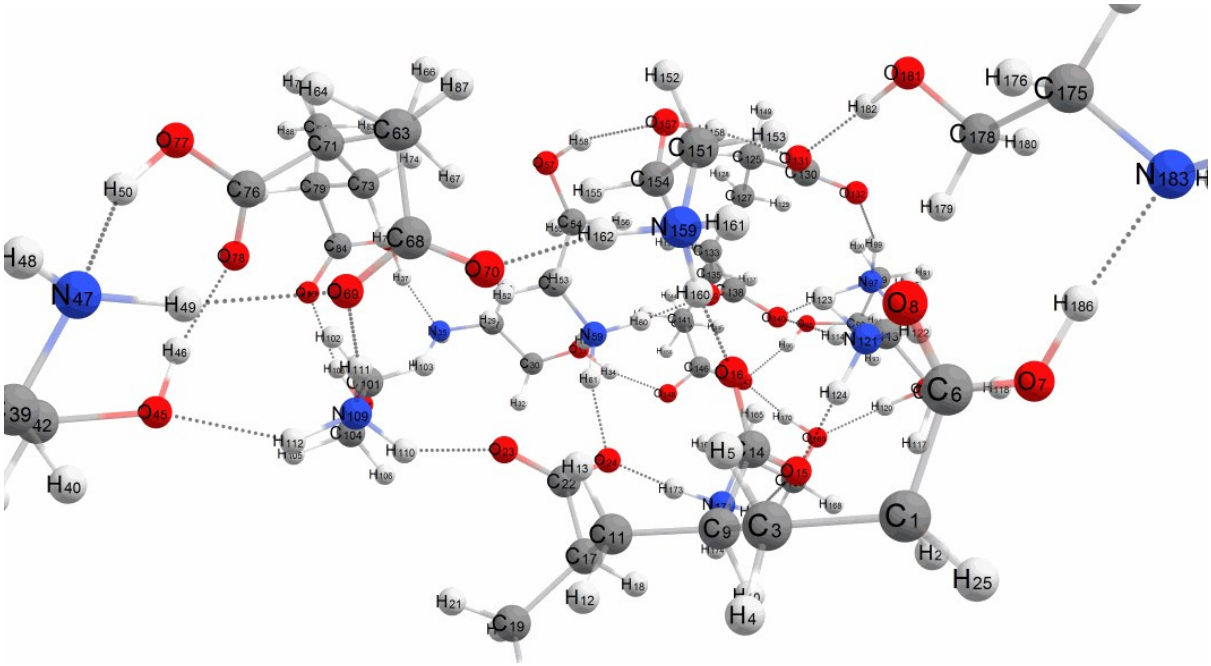

Figure S7. DFT simulation of hydrogen bonds in D-PAA/C-EA. 3D network would form between molecules chain A ($C_{1,3,9,11,17}$), chain B ($C_{63,65,71,73,79}$), and chain C ($C_{125,127,133,135,141}$).

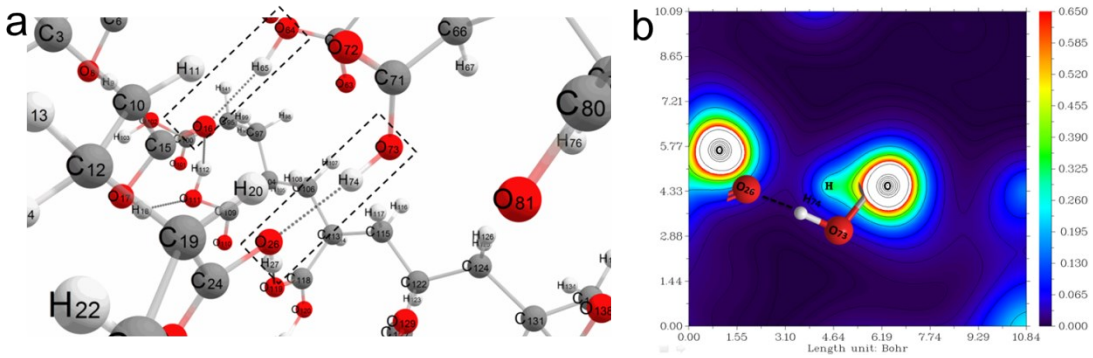

Figure S8. (a) Hydrogen bonds simulation in PAA. (b) Electrons density contour map of intermolecular hydrogen bonds in PAA.

Table S2. Classification of different hydrogen bonds

Type	Electrons density (a.u.)	E_{HB} (Kcal/mol)
-NH_3^+···OH	0.0479305475	-9.95005
-C=O···HO	0.0432948857	-8.91592
-OH···OH	0.0362164993	-7.33688
-COOH···HOOC	0.0246857680	-4.76460

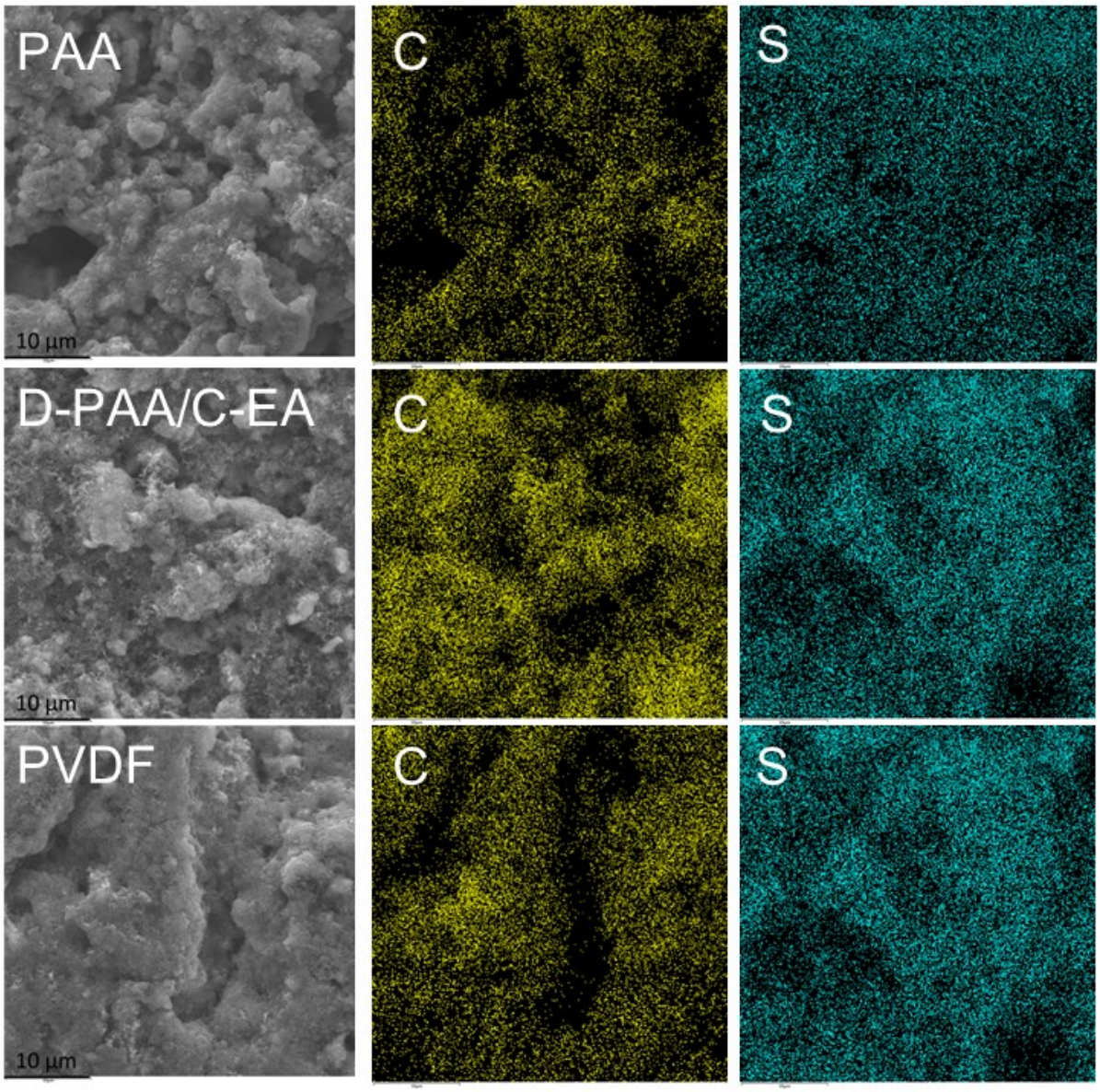

Figure S9. EDX elemental mappings of C and S in cathodes with PVDF, PAA, and D-PAA/C-EA binders.

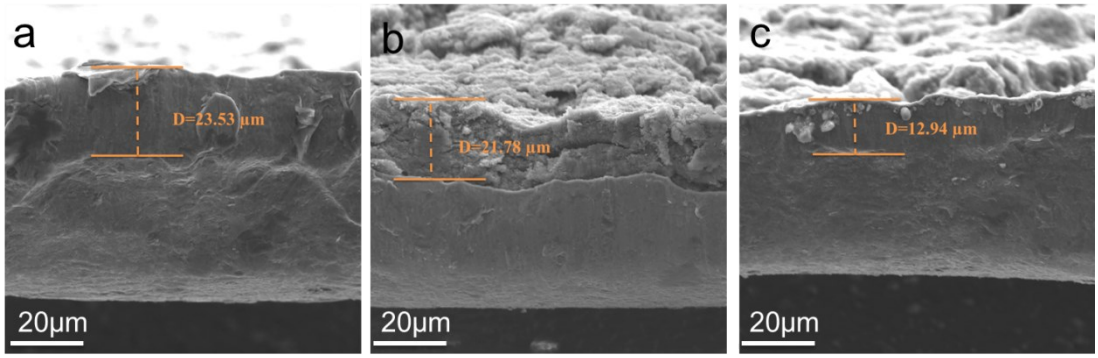

Figure S10. The cross-sectional morphologies of (a) PAA, (b) D-PAA/C-EA, (c) PVDF-based cathodes.

$$\text{cathode porosity} = \left\{1 - \frac{\frac{P_{act}}{TD_{act}} + \frac{P_{AB}}{TD_{AB}} + \frac{P_{binder}}{TD_{binder}}}{\frac{100}{CD_{ele}}}\right\} * 100\%$$

Where, P_{act}, P_{AB}, and P_{binder} are the proportion of active material (sulfur-based composites), conductive agent (AB) and binder (PA, D-PAA/C-EA, and PVDF) by mass. TD_{act}, TD_{AB} and TD_{binder} are the true densities of the active material (sulfur-based composites), conductive agent (super P) and binder, which are measured by the true density meter (AccuPyc 1330). The ture densities for KB/S, AB, PAA, D-PAA/C-EA and PVDF are 1.9508, 1.8638, 1.5070, 1.0105 and 1.7789 g cm^{-3}, respectively. CD_{ele} is the compact density of the electrode (without current collector) from SEM measurement, which is 0.7496, 0.4858 and 0.8177 g cm^{-3} for the electrodes with PAA, D-PAA/C-EA, and PVDF binder, respectively.[1]

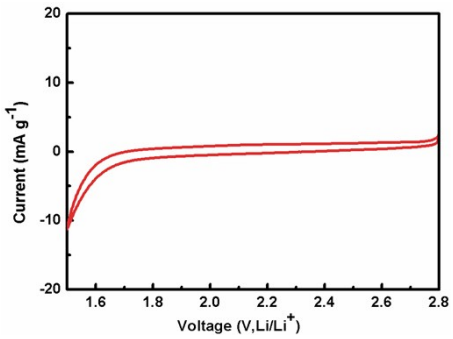

Figure S11. CV curves of the blank D-PAA/C-EA binder at a scan rate of 1 mV s^{-1}.

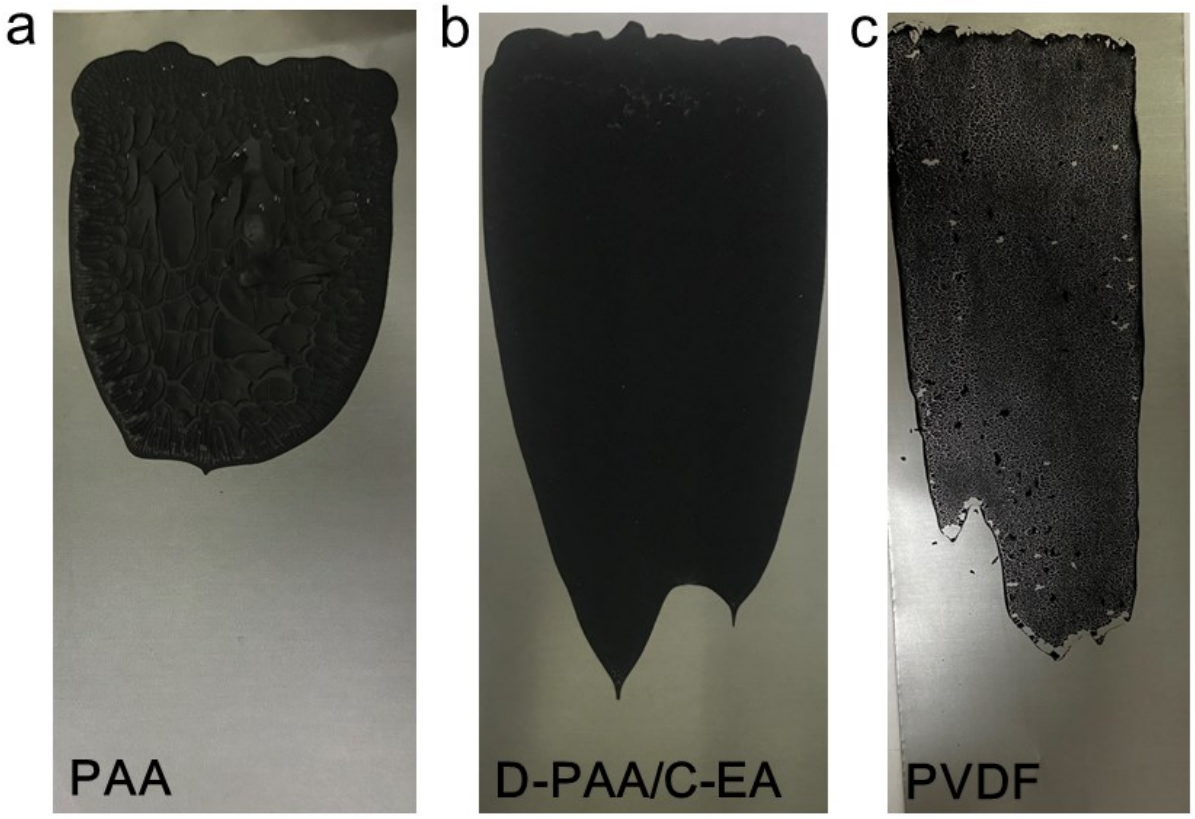

Figure S12. Photographs of the dried cathodes with (a) PAA, (b) D-PAA/C-EA, and (c) PVDF at a high sulfur loading of 3 mg cm^{-2}.

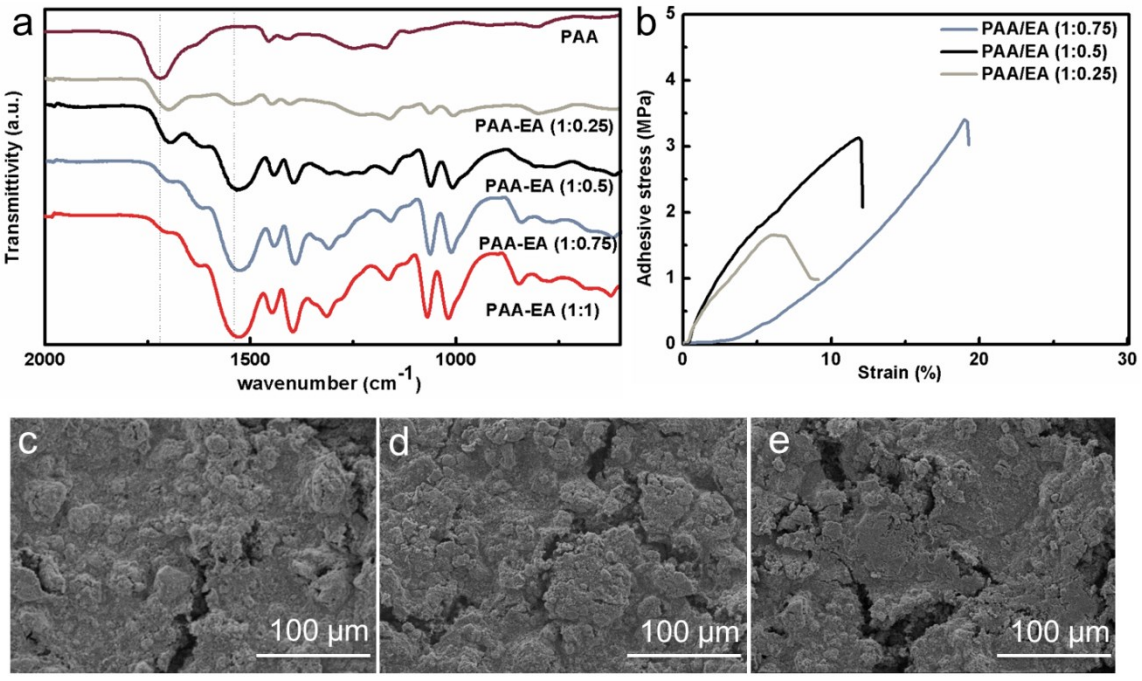

Figure S13. (a) FTIR spectra and (b) stress-strain (pull-off adhesion test) plot D-PAA/C-EA

binders with different PAA/EA ratio. (c-e) SEM images of the surface of cathodes (sulfur loading: 1 mg cm^{-2}) fabricated using (c) PAA-EA (1:0.25), (d) PAA-EA (1:0.5), and (e) PAA-EA (1:0.75).

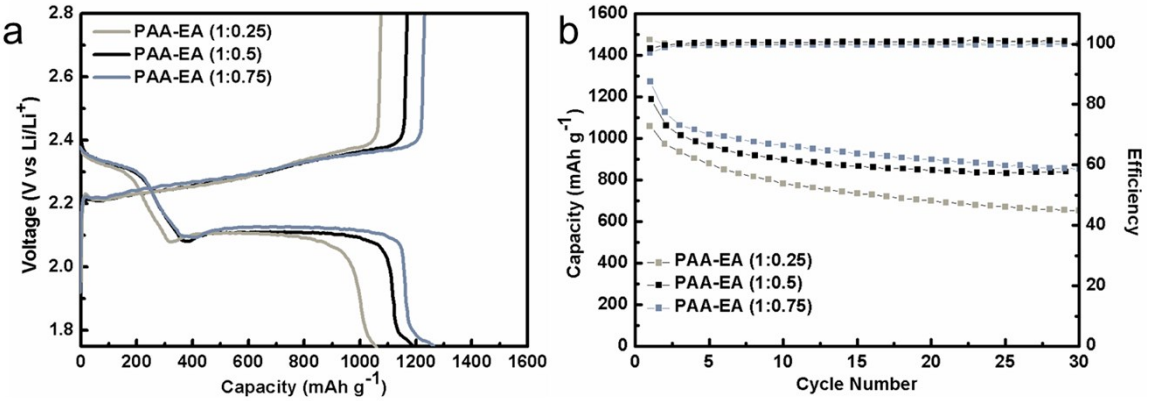

Figure S14. Voltage profile of the 1st cycle (a) and cycling performance (b) of different ration of (PAA/EA) sulfur cathode (1 mg cm^{-2}).

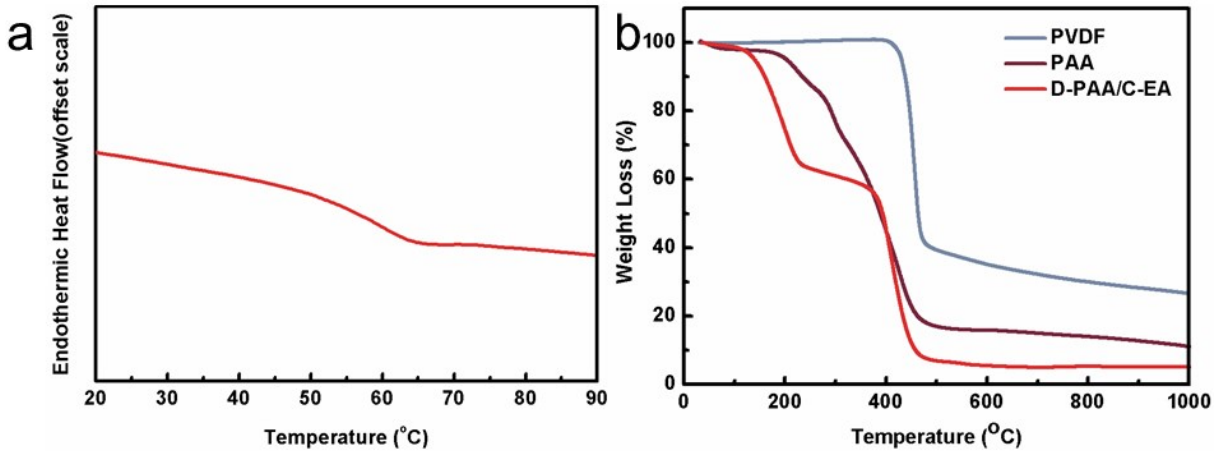

Figure S15. (a) DSC curve of D-PAA/C-EA and (b) TG measurement of PAA, D-PAA/C-EA, and PVDF.

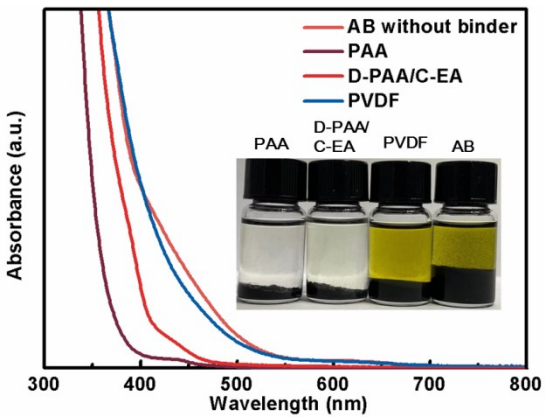

Figure S16. UV-vis spectra and photographs of the Li_2S_6 (2 mM) solution after soaking

by different AB/binder composites.

Table S3 Comparison of selected binders for Li-S batteries

Binders	S loading (mg cm^{-2})	Initial cycle discharge (mAh g^{-1})	cycles	Capacity Fading per Cycle (%)	High rate performance (mAh g^{-1})	E/S (μL mg^{-1})	Ref.
PVP	0.5-0.8	~1260.0 (0.2 C)	200	0.17	-	-	2
PVP/PEO	0.5-0.8	~1380.0 (0.2 C)	200	0.15	-	-	2
CMC/SBR	0.5-0.8	~1210.0 (0.2 C)	200	-	-	-	2
GOPAA	0.8	820.0 (0.5 C)	100	0.22	464.0 (3.0 C)	20	3
PAA	0.8	607.0 (0.5 C)	100	0.26	310.0 (3.0 C)	20	3
PPA	1.2-1.5	910.0 (0.5 C)	100	0.16	480.0 (3.0 C)	-	4
APP	2.0-3.0	753.0 (0.5 C)	500	0.126	-	10	5
L-AG	1.0	~1210.0 (1.0 C)	200	0.26	500.0 (2.0 C)	17	6
PSPEG	2.0	1156.0 (0.5 C)	500	0.06	-	7	7
TA/PEO	2.0 and 5.0	599.3 (2.0 mg cm^{-2}, 0.5 C)	150	0.17	438.0 (2.0 mg cm^{-2}, 3.0 C)	10	8
WPU/PAA/GN	2.3	1243.0 (0.5 C)	150	0.06	695.0 (3.0 C)	20	9
DICP	1.0 and 4.5	1035.0 (1.0 mg cm^{-2}, 0.5 C)	200	0.12	701.0 (1.0 mg cm^{-2}, 3.0 C)	20	10

	1.0	1217.4 (0.2 C)	300	0.13	638.6 (1.0	
This work	3.0	1210.3 (0.2 C)	100	0.2	mg cm^{-2}, 10.0	8
	5.0	610.0 (0.2 C)	100	0.016	C)	

Reference:

1. L. Wang, Y.-H. Song, B.-H. Zhang, Y.-T. Liu, Z.-Y. Wang, G.-R. Li, S. Liu and X.-P. Gao, *ACS Applied Materials & Interfaces*, 2020, **12**, 5909-5919.
2. M. J. Lacey, F. Jeschull, K. Edstrom and D. Brandell, *Journal of Power Sources*, 2014, **264**, 8-14.
3. G. Y. Xu, Q. B. Yan, A. Kushima, X. G. Zhang, J. Pan and J. Li, *Nano Energy*, 2017, **31**, 568-574.
4. W. Chen, T. Y. Lei, T. Qian, W. Q. Lv, W. D. He, C. Y. Wu, X. J. Liu, J. Liu, B. Chen, C. L. Yan and J. Xiong, *Advanced Energy Materials*, 2018, **8**.
5. G. M. Zhou, K. Liu, Y. C. Fan, M. Q. Yuan, B. F. Liu, W. Liu, F. F. Shi, Y. Y. Liu, W. Chen, J. Lopez, D. Zhuo, J. Zhao, Y. C. Tsao, X. Y. Huang, Q. F. Zhang and Y. Cui, *Acs Central Sci*, 2018, **4**, 260-267.
6. Q. Qi, Y. Q. Deng, S. C. Gu, M. Gao, J. Y. Hasegawa, G. M. Zhou, X. H. Lv, W. Lv and Q. H. Yang, *Acs Applied Materials & Interfaces*, 2019, **11**, 47956-47962.
7. F. L. Zeng, N. Li, Y. Q. Shen, X. Y. Zhou, Z. Q. Jin, N. Y. Yuan, J. N. Ding, A. B. Wang, W. K. Wang and Y. S. Yang, *Energy Storage Materials*, 2019, **18**, 190-198.
8. H. Zhang, X. Hu, Y. Zhang, S. Wang, F. Xin, X. Chen and D. Yu, *Energy Storage Materials*, 2019, **17**, 293-299.
9. M. Y. Zheng, X. M. Cai, Y. F. Tan, W. Q. Wang, D. Y. Wang, H. J. Fei, P. Saha and G. C. Wang, *Chem Eng J*, 2020, **389**.
10. Z. Liu, X. He, C. Fang, L. E. Camacho‐Forero, Y. Zhao, Y. Fu, J. Feng, R. Kostecki, P. B. Balbuena and J. Zhang, *Advanced Functional Materials*, 2020, 2003605.